CALIFORNIA STATE UNIVERSITY, NORTHRIDGE

AIRCRAFT GROUND STATION COMMUNICATIONS TEST ENVIRONMENT CHARACTERIZATION

A project submitted in partial fulfillment of the requirements
For the degree of Master of Science
In Electrical Engineering

By
Shannon Porter

May 2012

The project report of Shannon Porter is approved:

_____	_____
Mr. James Flynn	Date
_____	_____
Dr. Sembiam Rengarajan	Date
_____	_____
Dr. Sharlene Katz, Chair	Date

California State University, Northridge

TABLE OF CONTENTS

LIST OF TABLES

LIST OF FIGURES

ABSTRACT

AIRCRAFT GROUND STATION COMMUNICATIONS TEST ENVIRONMENT CHARACTERIZATION

By
Shannon Porter

Master of Science in Electrical Engineering

This project report presents the concept, rationale, and results for the environment characterization pertaining to an aircraft communications ground test. The overall objective of this effort was to explore the supposition that an aircraft communications ground test with a relatively close range can adequately represent ground to air communications with a slant range of 0.4 nautical miles. Initial preliminary test analysis had presumed a single direct transmission path for calculations of both a close 50ft range and 0.4Nmi slant range. This effort involved gathering data from electromagnetic software simulations that were representative of a ground test with a close range of approximately 50ft and of a ground to air communications scenario with a slant range of 0.4 nautical miles. Simulations including scattering objects, transmissions, reflections, diffractions, and multiple paths were planned to complete a more comprehensive evaluation of both scenarios.

CHAPTER 1: INTRODUCTION

1.1 General

This project report presents the concept, rationale, and results for the environment characterization pertaining to an aircraft communications ground test. The overall objective of this effort was to explore the supposition that an aircraft communications ground test with a relatively close range can adequately represent ground to air communications with a slant range of 0.4 nautical miles. This effort involved gathering data from electromagnetic software simulations that were representative of a ground test with a close range of approximately 50ft and of a ground to air communications scenario with a slant range of 0.4 nautical miles. Objects in both scenarios were assumed to be static. These two scenarios are shown in the figure below.

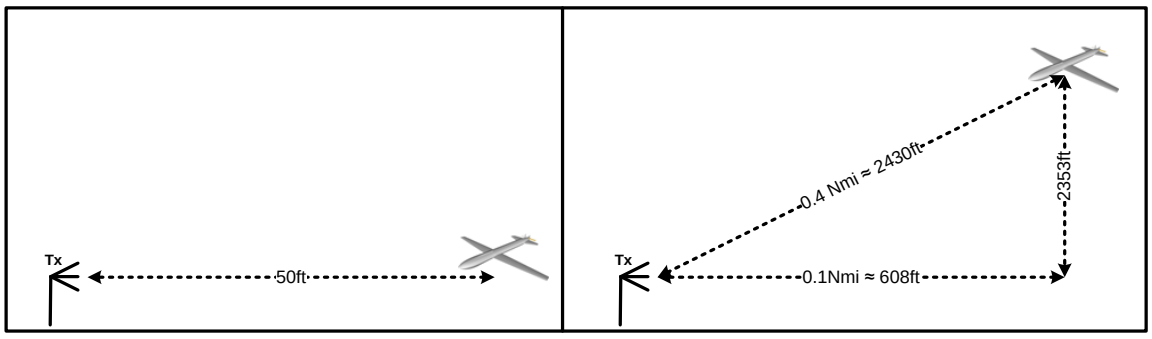

Figure 1: Simulation Scenarios

1.2 Background

This project involved a preliminary effort to support an aircraft communications ground test. The aircraft communications ground test entails the characterization of UHF communications between the aircraft and ground station via links for data or voice. A ground test with 50ft range between transmitting antenna and receiving antenna was planned in lieu of the flight representative 0.4Nmi range. A ground test was planned instead of a flight test to reduce overall cost. A shorter range was planned according to the availability of test area with line-of-sight propagation free from terrain and building obstructions and with accessibility for personnel and equipment.

A preliminary analysis and comparison of link budgets for both ranges was used to compensate for differences in free space path loss. While the UHF communications range varied from 225MHz to 400MHz, the specific value of 395MHz was used for preliminary analysis calculations. The analysis presumed a single direct transmission path for calculations of both the 50ft range and 0.4Nmi slant range. For the 50ft range, power received via the aircraft antenna was fixed according to what was calculated using a standard link budget for single ray approximation for the 0.4Nmi range. Transmitter input power for the 50ft range was then varied from that of the 0.4Nmi range to compensate for differences in free space loss. The accuracy of this input power variation calculated using a single ray approximation was explored using simulations.

Project assets included the aircraft, a ground station, and power and cooling equipment. Simulations including scattering objects, transmissions, reflections, diffractions, and multiple paths were planned to complete a more comprehensive evaluation of both scenarios.

1.3 Modeling and Simulation

Modeling of the environment and simulation of propagation was completed using a ray-based electromagnetic analysis tool, Remcom's XGtd. This tool is based upon the Geometric Theory of Diffraction, GTD, a high frequency, field-based method of computational electromagnetics. Use of high frequency methods are appropriate for objects that are large in size compared to a wavelength.(Stutzman, 427) For UHF communications ranging from 225MHz to 400MHz, the sizes of project objects were large compared to the corresponding wavelengths varying from 0.75 to 1.33 meters.

CHAPTER 2: THEORY

2.1 Link Budget Analysis

For an aircraft communications ground test, the ground station and aircraft were proposed to be located on the ground approximately 50 feet apart. To simulate a measurement of 0.4 nautical miles slant range, the transmitting power was planned to be varied to compensate for the differences in free space loss. Input power level and test equipment insertion losses had already been taken into account for the planned effective isotropic radiated power (EIRP) of 39.1 dBm. The variation in power to compensate for the differences in range distances was calculated using the following equations and is shown in the following figure.

$$P_{T,50ft} + L_{F,50ft} = P_{T,0.4Nmi} + L_{F,0.4Nmi}$$

$$\rightarrow P_{T,50ft} = P_{T,0.4Nmi} + L_{F,0.4Nmi} - L_{F,50ft}$$

$$\text{where } L_F = -20 * log\left(\frac{4\pi R}{\lambda}\right)$$

$$\rightarrow P_{T,50ft} = 39.1dBm - 20log\left(\frac{0.4Nmi}{50ft}\right) \approx 5.3dBm$$

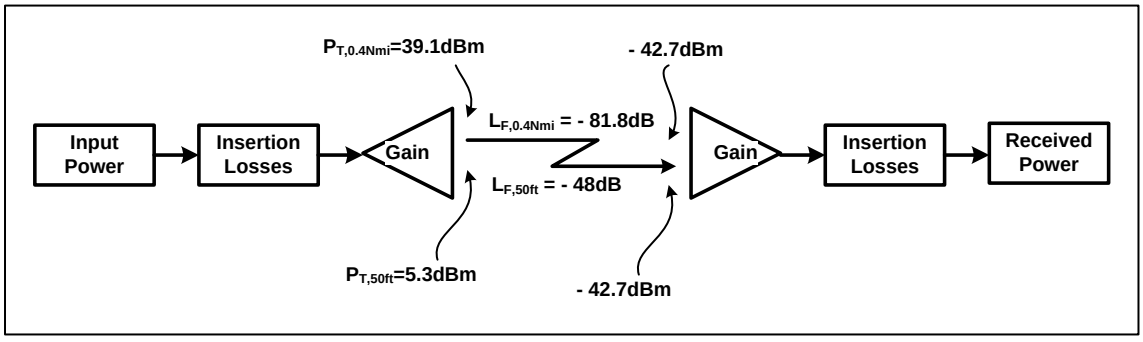

Figure 2: Link Budgets for 50ft and 0.4Nmi Ranges

The link budget analysis was based upon the transmission of a single ray from the transmitting antenna to the receiving antenna while only taking into account the free-space path loss. Additional considerations were that the actual placement of the aircraft for a ground test would result in an error factor in the range distance and that the location of the antenna on the aircraft was estimated. In order to compensate for these, the entire region in which the aircraft antenna was located was evaluated using receiver grids in the simulation.

2.2 Transverse and Longitudinal Probing Methods

The receiver grids described in section 3.6 were positioned in three planes to effect transverse and longitudinal probing methods to explore the significance of scattering by receiver position. One receiver grid was positioned transverse to the direction of propagation, another was positioned longitudinal to the direction of propagation, and a third was positioned horizontally combining both the transverse and longitudinal positioning. Received power was expected to only have small changes in the absence of significant scattering. This methodology is similar to the Antenna-Pattern-Comparison Method.[IEEE, 37]

2.3 Spherical Wave Front

In the simulation, three receiver grids positioned in three planes provided the power received into the antennas for moderately varying distances from the transmitting antenna. Frequently, the wave front of an impinging source is approximated as planar when in actuality the wave front is spherical. The spherical wave front results in varying path lengths and phase variation as shown in the following figure.[Hollis, 14-7]

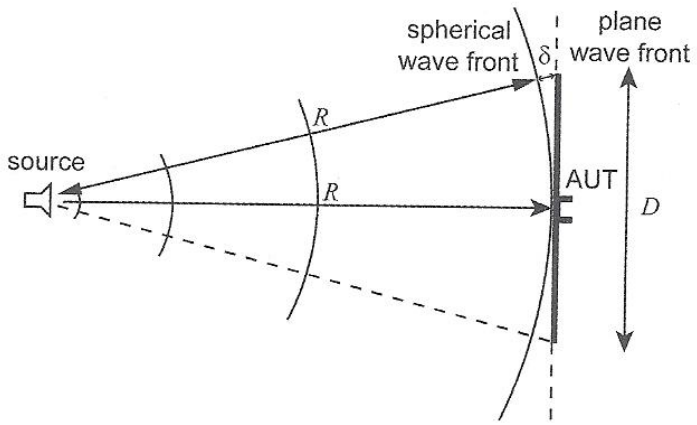

Figure 3: Spherical and Plane Wave Fronts

The variation in path length was determined using the following equation.

$$\boldsymbol{\delta = \left[R^2 + \left(\frac{D}{2}\right)^2\right]^{1/2} - R}$$

For receiver grids with a maximum length of approximately D = 10ft and range of R=50ft, the path variation was a maximum of 0.25ft resulting in a very small additional path loss of up to -0.005dB at the maximum and minimum frequencies of 225MHz and 400MHz. For receiver grids with a maximum length of approximately D = 10ft and range of R=0.4Nmi, the path variation was 0.005ft resulting in an even smaller additional path loss at both frequencies.

Given that the additional path loss contributed by the plane wave front assumption was very slight, using receiver grids for evaluation made no significant impact on the accuracy of the data calculated by a single path analysis. It did provide additional insight into the summing of multiple paths in the region resulting from scattering effects.

2.4 Fresnel Zone Analysis

While the transmit power was planned to be adjusted to compensate for free space loss, there was no additional compensation for interference from the ground or other obstacles that would not be as significant factors in the air. Fresnel Zone analysis shows the regions of constant phase for which the ground and obstacles would present constructive and destructive interference. While particular care is ideally given to avoid locating obstacles within these regions, complete avoidance may be impractical for an actual test. Cables and ducts for support carts have physical constraints with regard to length. In addition, the aircraft on which the receiving antenna was located is also an object whose features are in close proximity and contribute to scattering effects. Fresnel Zone center, length, and width were determined using the following functions(Hemming 183) where N is the Nth Fresnel Zone.

$$F_1 = \left[\frac{N\lambda}{2R} + \sec(\varphi)\right]$$

where the grazing angle $\varphi = tan^{-1}\left[\frac{h_r + h_t}{R}\right]$

$$F_2 = (h_r^2 - h_t^2)/[(F_1^2 - 1)R^2]$$

$$F_2 = (h_r^2 + h_t^2)/[(F_1^2 - 1)R^2]$$

Center: $C_N = R(1 - F_2)/2$

Length: $L_N = RF_1(1 + F_2^2 - 2F_3)^{1/2}$

Width: $W_N = R[(F_1^2 - 1)(1 + F_2^2 - 2F_3)]^{1/2}$

The Fresnel Zones were calculated for the minimum and maximum frequencies of 225MHz and 400MHz in consideration of the 50ft range and the 0.4Nmi slant range. As shown in the following figure and the corresponding figures in the appendices, the Fresnel zones for the 50ft range encompass a significant portion of the ground area between the transmitting and receiving antennas. The Fresnel zones for the 0.4Nmi slant range only encompass a relatively small area about the transmitting antenna, however. Hence, the scattering effects of objects within the Fresnel Zones for the 50ft range were predicted to be more significant than those for the 0.4Nmi slant range.

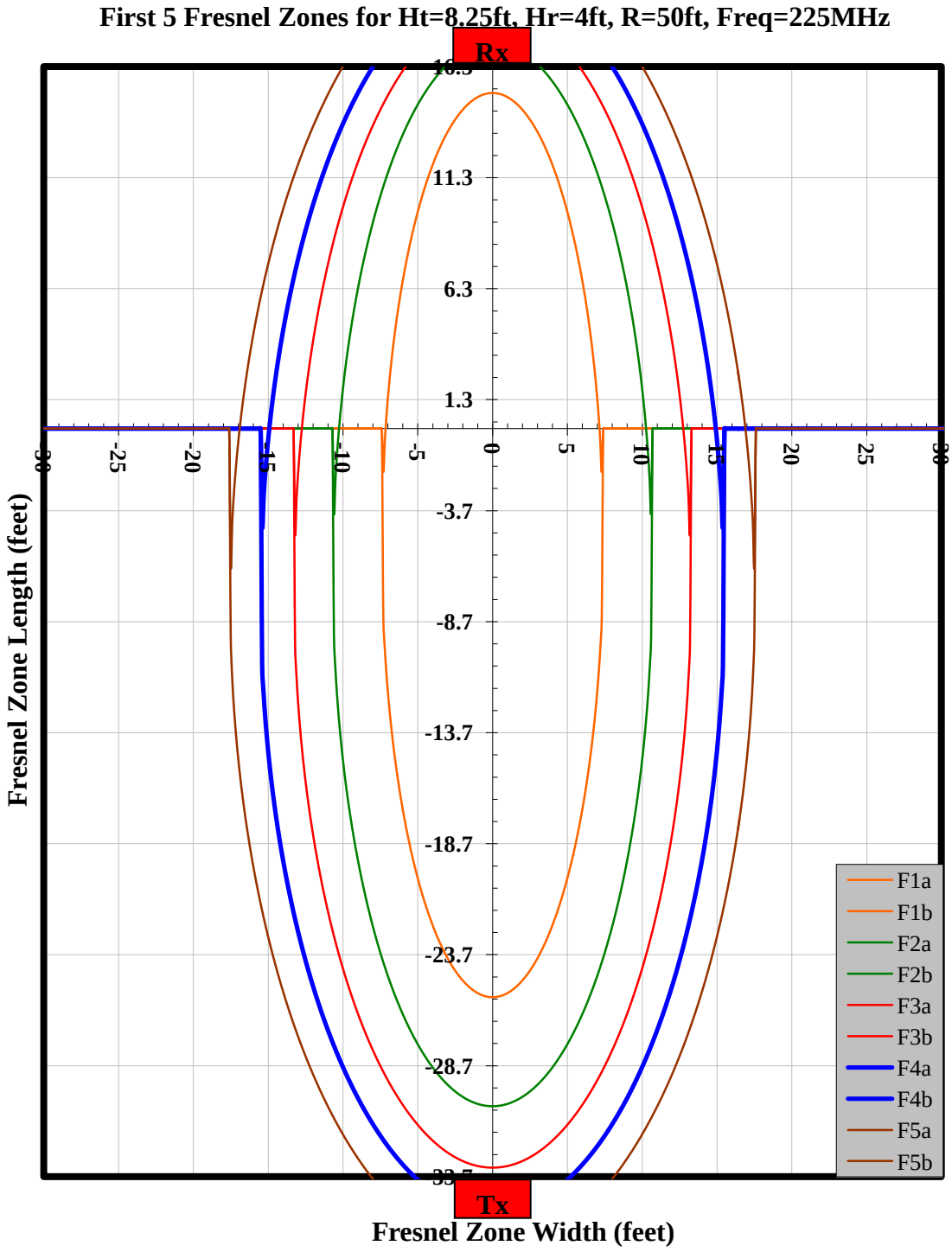

Figure 4: Fresnel Zones for 50ft Range at 225MHz

CHAPTER 3: SIMULATION PARAMETERS

3.1 General

Software simulations were run to represent both a ground test environment and a ground-to-air environment at actual slant range including known obstacles. Parameters for the simulations were determined using typical resources for aircraft communications tests.

3.2 Materials

Generic material types were used for software simulation objects, called features within the software program. Material properties utilized by the software include either relative permittivity and conductivity or reflection and transmission coefficients. Specific values for the materials used for this project are shown in the following table.

Table 1: Simulation Materials

Material	Relative Permittivity, ϵ	Conductivity, σ(S/m)	Transmission Coefficients	Reflection Coefficients
Soil (dry)(Cheng, 675)	3-4	10^{-5}	-	-
Perfect Electrical Conductor (PEC) (XGTD, 50)	-	-	0	
Advanced Composite (Graphite Fiber Reinforced Plastic)	4.25(Felbecker, 4)	$5.56*10^{4}$ (Evans, 14)	-	-
Free Space(XGTD, 51)	-	-	1	0

3.3 Features

Objects within the simulation, called features, included the aircraft, a ground station, a cooling cart, a power cart, and the earthen ground surface. A commercially available computer-aided-drafting model of an actual aircraft under test was imported into the software. The model was comprised of 2697 faces which were associated with the previously defined advanced composite material. The faces were set as doubled-sided since transmissions were included in the simulation runs. The ground station, cooling cart, and power cart were approximated as rectangular prisms. Their faces were set as

double-sided and as the predefined perfect electrical conductor material since they were mostly metal.

Table 2: Simulation Features

Feature	Dimensions	Material	Relative Location
Aircraft	Wingspan: ~133ft Length: ~48ft	Advanced Composite	50ft and 0.4Nmi slant range from ground station
Ground Station	L*W*H 10.83ft*8ft*8.25ft	PEC	Simulation origin
Air Cooling Cart	L*W*H 11.4ft*6.4ft*6.5ft	PEC	2-3ft beyond left wingtip
Power Cart	L*W*H 50in*22.75in*21in	PEC	~20ft left of fuselage
Earth	Flat surface	Soil (dry)	Ground

3.4 Waveform

The waveform was modeled as a sinusoid with carrier frequencies of 225, 395, and 400 MHz, bandwidth of 0.025 MHz, and phase of 0 degrees. 225 MHz and 400 MHz were the maximum and minimum of the frequency range, while 395MHz was called out for the planning of a particular communications test.

3.5 Antennas

Typical military UHF voice systems operate within the 225-400MHz frequency range and are vertically polarized. Antennas for these systems are omnidirectional and frequently monopoles or their variants, such as blade antennas which offer low drag (Volakis 40-2, 40-15). Consequently, the project aircraft antennas were modeled as monopoles which were readily defined within the software. Their lengths were much less than one wavelength and set to 10 inches. The maximum gain was incorporated with the input power and insertion losses providing 39.1 dBm EIRP. The receiver threshold was set as -250dBm thereby setting a lower limit for ray paths in order to speed software calculation time. A 3-D graphical representation of the antenna pattern is shown in the figure below.

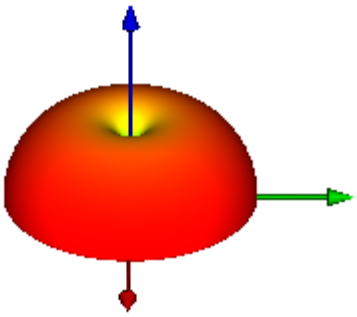

Figure 5: Antenna Pattern

3.6 Transmitter and Receivers

The transmitting antenna was modeled as a point on the top face of the ground station as shown in the figure below. The aircraft nose faced the ground station and transmitting antenna. Due to contractual reasons, the aircraft model was rendered invisible for the purpose of this report. However, reflections caused by the aircraft are evident in this and other figures.

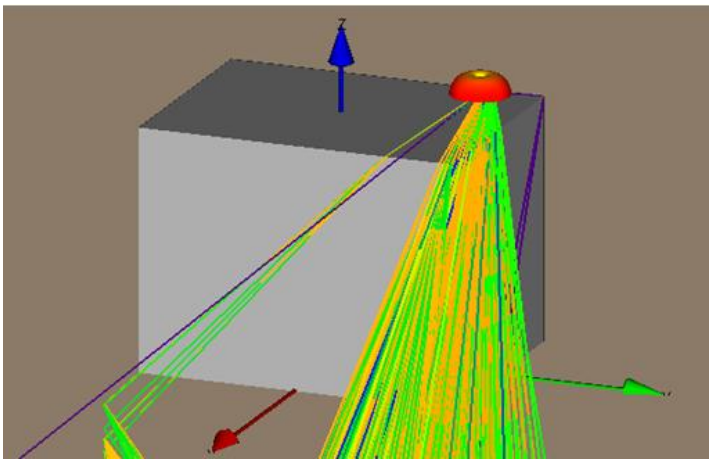

Figure 6: Transmitting Antenna on Ground Station

In consideration of the variation of power level received by distance and limited information on the precise positioning of the receiving antenna, the antenna was modeled as receiver grids underwing on the starboard side of the aircraft in a fashion similar to field probe measurements. A horizontal grid consisted of 121 receiving antennas, a longitudinal grid consisted of 33 receiving antennas, and a transverse grid consisted of 30 receiver antennas. The longitudinal and transverse grids had fewer antennas compared to the horizontal grid since their area was limited by the ground surface and the aircraft wing. Each of these receiving antennas represented a data point for analysis. The

following figure shows a visual rendering of the receiver grids used for analysis. The longitudinal grid is highlighted as a cream color while the transverse and horizontal grids are red. The individual receiving antennas are shown as boxes. The box size and spacing was specified for visual purposes only and does not represent the collection area of each.

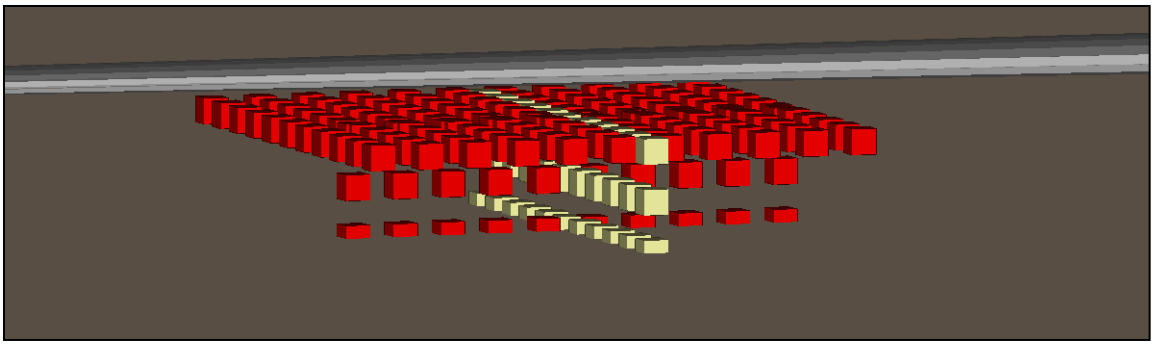

Figure 7: Receiver Grid Orientation

3.7 Study Area

Finally, the study area which defined the project area in which to calculate the simulation was defined. The study area for this project was automatically set to encompass all defined features. In addition, the ray-spacing was defined for the study area in accordance with the software user manual guidance that angular ray spacing result in no more than 5.73ft of separation at the receiving antenna. In consideration of this guidance, the angular ray spacing was determined using the following equations.

$$Ray\ spacing = \theta_{50ft} < 2 * tan^{-1}\left(\frac{5.73ft/2}{50ft}\right) = 6.56°$$

$$Ray\ spacing = \theta_{0.4Nmi} < 2 * tan^{-1}\left(\frac{5.73ft/2}{2430ft}\right) = 0.14°$$

As a conservative measure, both maximum ray spacing angles were decreased by a factor of 6, resulting in Θ_{50ft} equal to 1° and $\Theta_{0.4Nmi}$ equal to 0.02°.

CHAPTER 4: DATA ACQUISITION

The ray paths from the transmitting antenna to all receivers given the prescribed angular spacing were determined by the software and rendered graphically. Scattering structures included various aspects of the aircraft, which was intentionally rendered as invisible in the following figure, as well as the earth surface. The figure shows scattering effects from the ground and aircraft fuselage and tail.

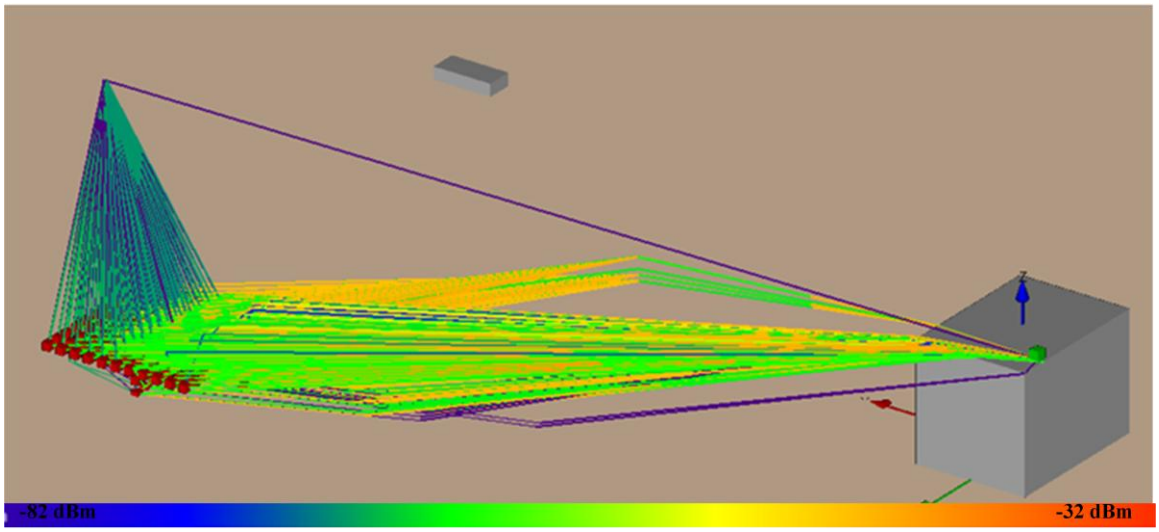

Figure 8: Propagation Paths for 50ft Range and 225MHz

In addition, the power contributed by each path was summed by the software to determine each receiving antenna's received power. The summation included phase information and was calculated according to the following equation

$$P_R = \frac{\lambda^2 \beta}{8\pi\eta_o}\left|\sum_{i=1}^{N_p}\left[E_{\theta,i}g_\theta(\theta_i,\phi_i) + E_{\phi,i}g_\phi(\theta_i,\phi_i)\right]\right|^2$$

where λ is the wavelength, η_o is the impedance of free space, β is the overlap of the frequency spectrum of the transmitted wave and the spectrum of the frequency sensitivity of the receiver, N_p is the number of paths, $E_{\theta,i}$ and $E_{\phi,i}$ are the theta and phi components of the electric field of the i^{th} path at the receiver point, $g(\theta,\phi)$ gives the directional arrival. (XGTD, 149) The received power was rendered graphically as well and is shown as shown in the following figure and in corresponding figures in the appendices.

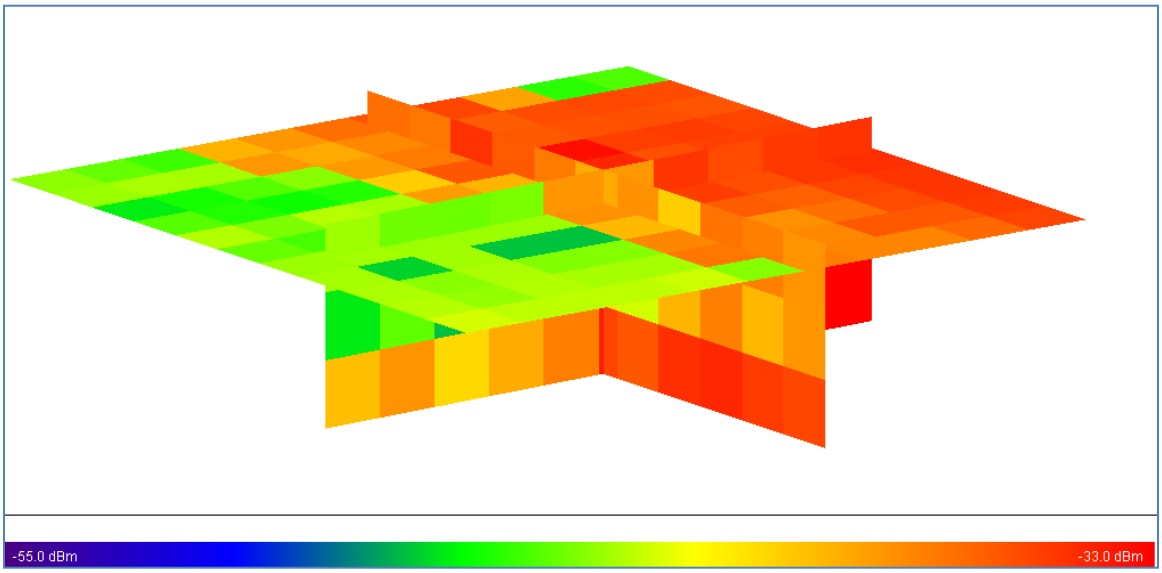

Figure 9: Received Power for 50ft Range and 225MHz

Finally, tabular data generated by the software to produce the graphical results was available in space delimited file format. The tabular data provided specific details including the total power received by each antenna, range distances for each antenna, the number of ray paths contributing to each total, and the types of electromagnetic environmental interaction of each path. The interactions included transmissions, reflections, and diffractions. The tabular data was analyzed as discussed in the analysis section of this report.

CHAPTER 5: ANALYSIS

5.1 Power Received vs. Distance

While the 50ft range and 0.4 Nmi slant range were planned, positioning the receiver grids with regards to proximity to other objects was not precise using the graphical user interface. Hence the center positioning of the receiver grids were not exactly at 50ft range and 0.4Nmi slant range. This was apparent in the sample plots of power versus distance for the 50ft range and 0.4Nmi slant range at 225MHz that follow. Similar plots for the additional frequencies are in the appendices.

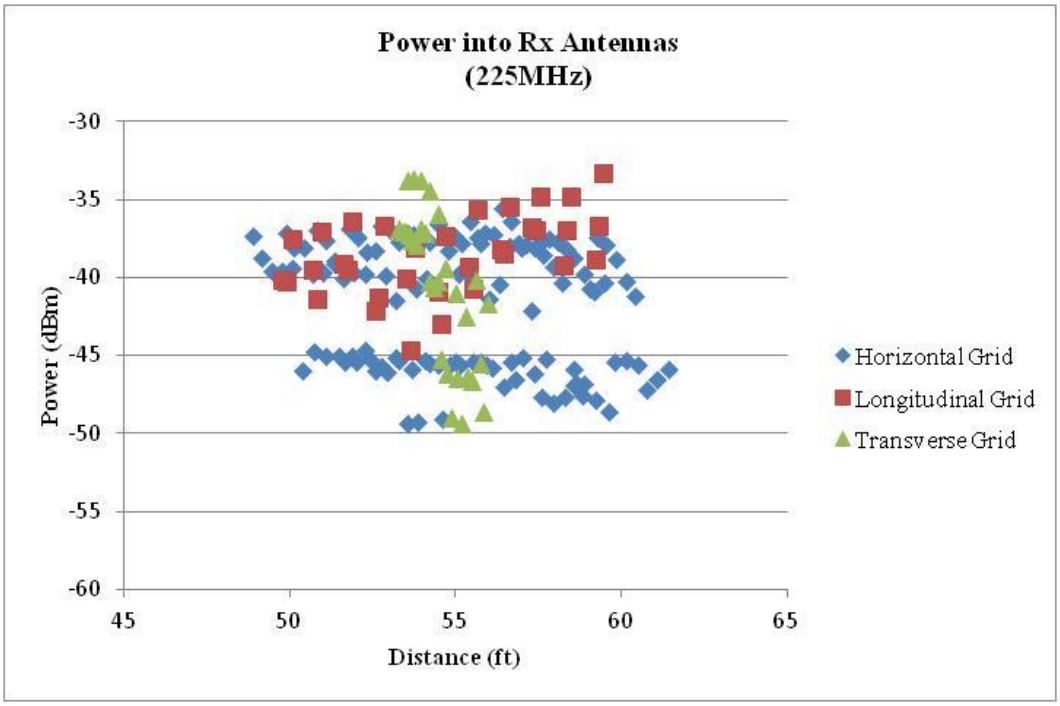

Figure 10: Power vs. Distance for ~50ft Range and 225MHz

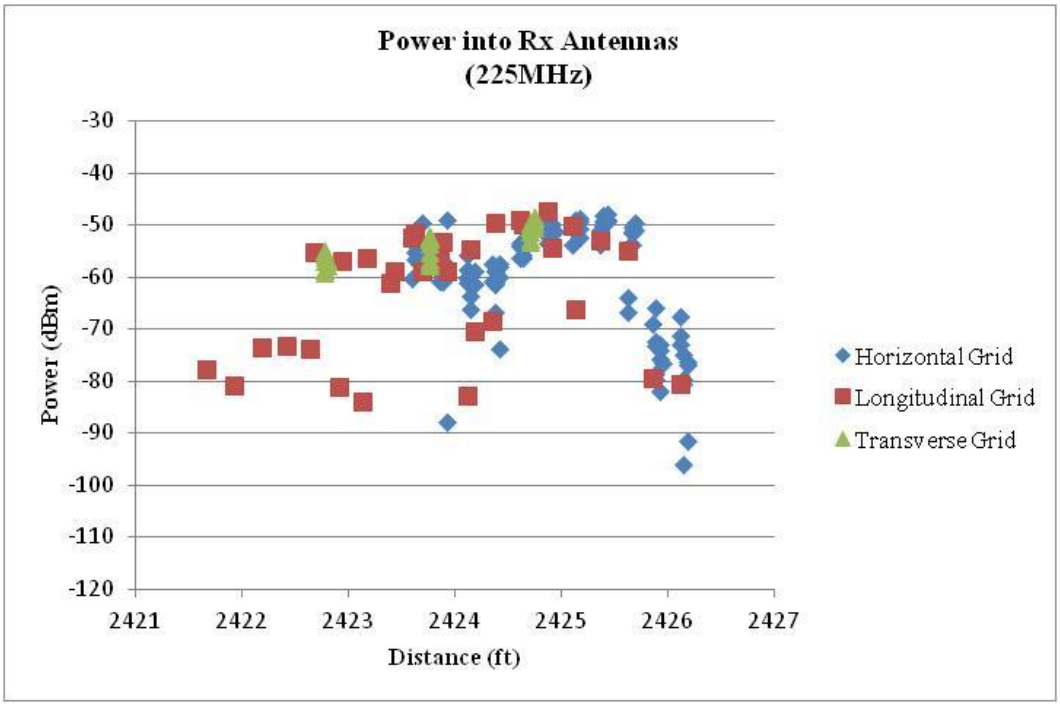

Figure 11: Power vs. Distance for ~0.4Nmi Slant Range and 225MHz

For the planned range of 50ft, the simulation range distances for all of the receivers varied from 48.1 to 61.4ft. For the planned range of 0.4Nmi, 2430ft, the simulation range distances for all of the receivers varied from 2421.7 to 2426.2ft according to the software. These deviations from the planned range distances directly affect the calculation of free space path loss and, consequently, the expected power received.

5.2 Revised Expected Power Levels

The variations in range altered the expected power levels which were revised by adjusting the free space path loss accordingly and are shown in the following tables. The originally planned calculations are also shown in the figures for comparison.

Table 3: Planned and Revised Expected Power Levels for 50ft Range

~50ft Range					
Range Description	**P_T (dBm)**	**Range (ft)**	**Frequency (MHz)**	**L_F (dB)**	**P_R (dBm)**
Planned	5.3	50	225	-43.1	-37.8
			395	-48.0	-42.7
			400	-48.1	-42.8

Simulation Minimum		48.1	225	-42.8	-37.5
			395	-47.7	-42.4
			400	-47.8	-42.5
Simulation Maximum		61.4	225	-44.9	-39.6
			395	-49.8	-44.5
			400	-49.9	-44.6

Table 4: Planned and Revised Expected Power Levels for 0.4Nmi Slant Range

~0.4Nmi Slant Range					
Range Description	**P_T (dBm)**	**Range (ft)**	**Frequency (MHz)**	**L_F (dB)**	**P_R (dBm)**
Planned	39.1	2430	225	-76.9	-37.8
			395	-81.8	-42.7
			400	-81.9	-42.8
Simulation Minimum		2421.7	225	-76.8	-37.7
			395	-81.7	-42.6
			400	-81.8	-42.7
Simulation Maximum		2426.2	225	-76.9	-37.8
			395	-81.8	-42.7
			400	-81.9	-42.8

The received power values for the originally planned calculations varied by up to approximately 2 dB in comparison to the revised values for the 50ft range. Little difference was shown in comparing the values for the 0.4Nmi slant range. This was not surprising considering the variation in range distance is very small compared to the actual range of 0.4Nmi.

5.3 Transverse and Longitudinal Probing

Receiver grids were used in the area of the antenna mounted upon the aircraft wing to illustrate the affects of scattering and reflections, if any. In the absence of scattering and reflections, the power received would be a function of the distance between the source and receiver with respect to the effective radiated power. However, scattering and reflections would result in significant deviations as evidenced by outliers from the general trend line. Such deviations are apparent in some of the following figures showing the data plotted for the horizontal receiver grids. Little deviation is evident for the approximate 50ft range plots which may be attributed to small variations in distance. The approximate 0.4Nmi range plots show deviations greater than 20dB towards the edges of the grids. These deviations show evidence of the effects of scattering and reflections. Similarly the longitudinal grids shown in the appendices reflect deviations

for the 0.4Nmi range, but not the 50ft range. However, the transverse grids shown in the appendices exhibit no such deviations for either range. Evaluating the data by horizontal, longitudinal, and transverse receiver grids shows that in general the received power is more affected by scattering and reflections for the 0.4Nmi range than the 50ft range. Frequency does not appear to be a significant factor for the deviations.

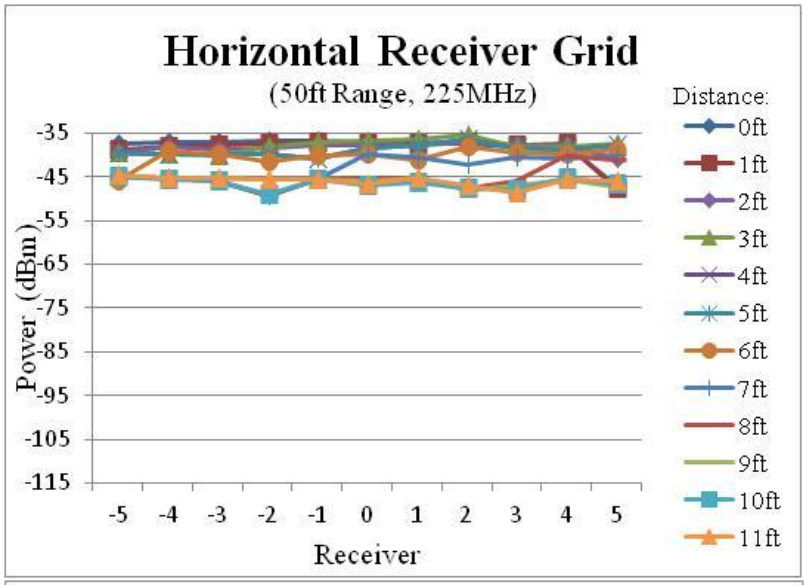

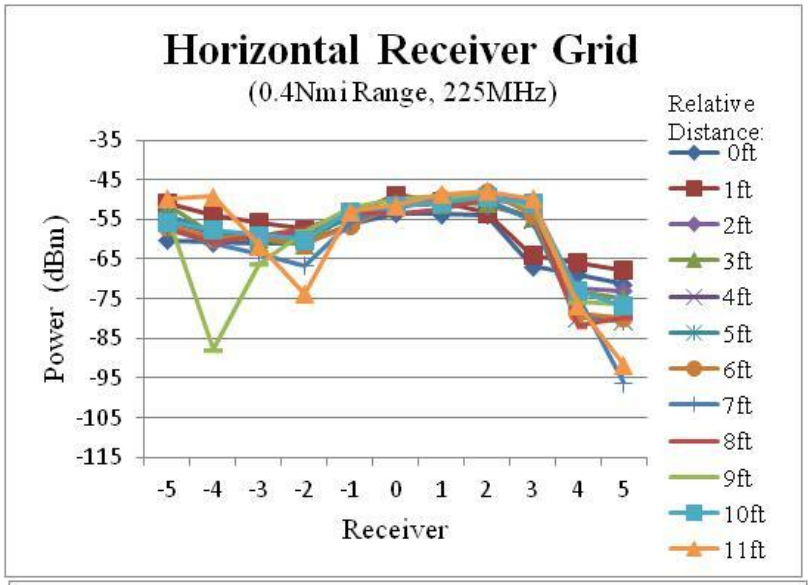

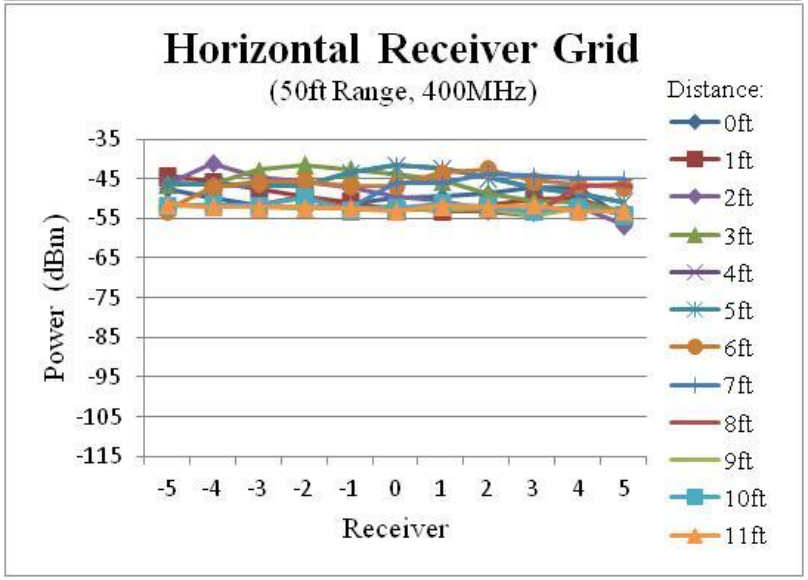

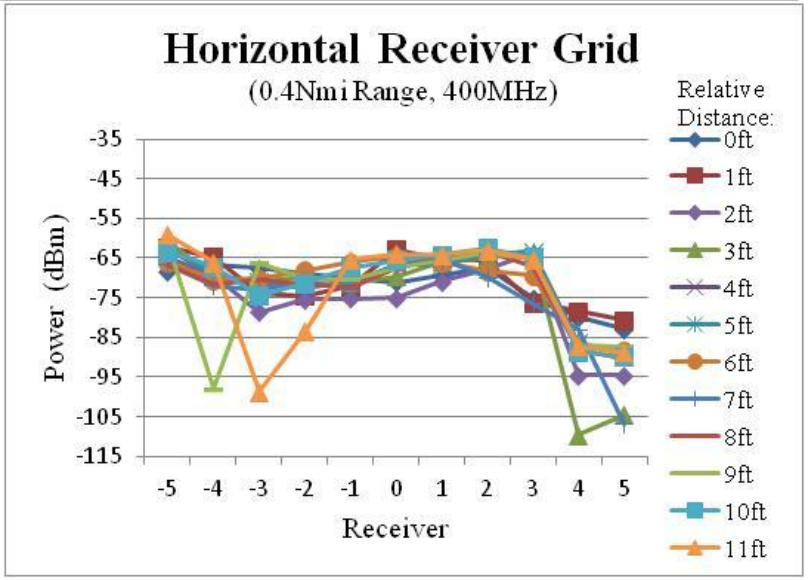

Figure 12: Data by Receiver Grids

5.4 Expected Versus Simulation Data

The simulation data for the 50ft range was plotted alongside the revised expected data for comparison in the figure below. The simulated received power levels for all three grids were combined by frequency. The minimum, maximum, average, and standard deviation were determined and plotted in a box and whisker format. The whiskers showed the minimum and maximum, while the box was centered at the average and extended both positively and negatively to reflect the standard deviation. Hence the box was determined using the following equation.

$$\bar{x} \pm \sqrt{\frac{\sum(x - \bar{x})^2}{n - 1}}$$

Where n is the sample size and "x-bar" is the sample mean. The expected data was plotted as a straight vertical line from minimum to maximum.

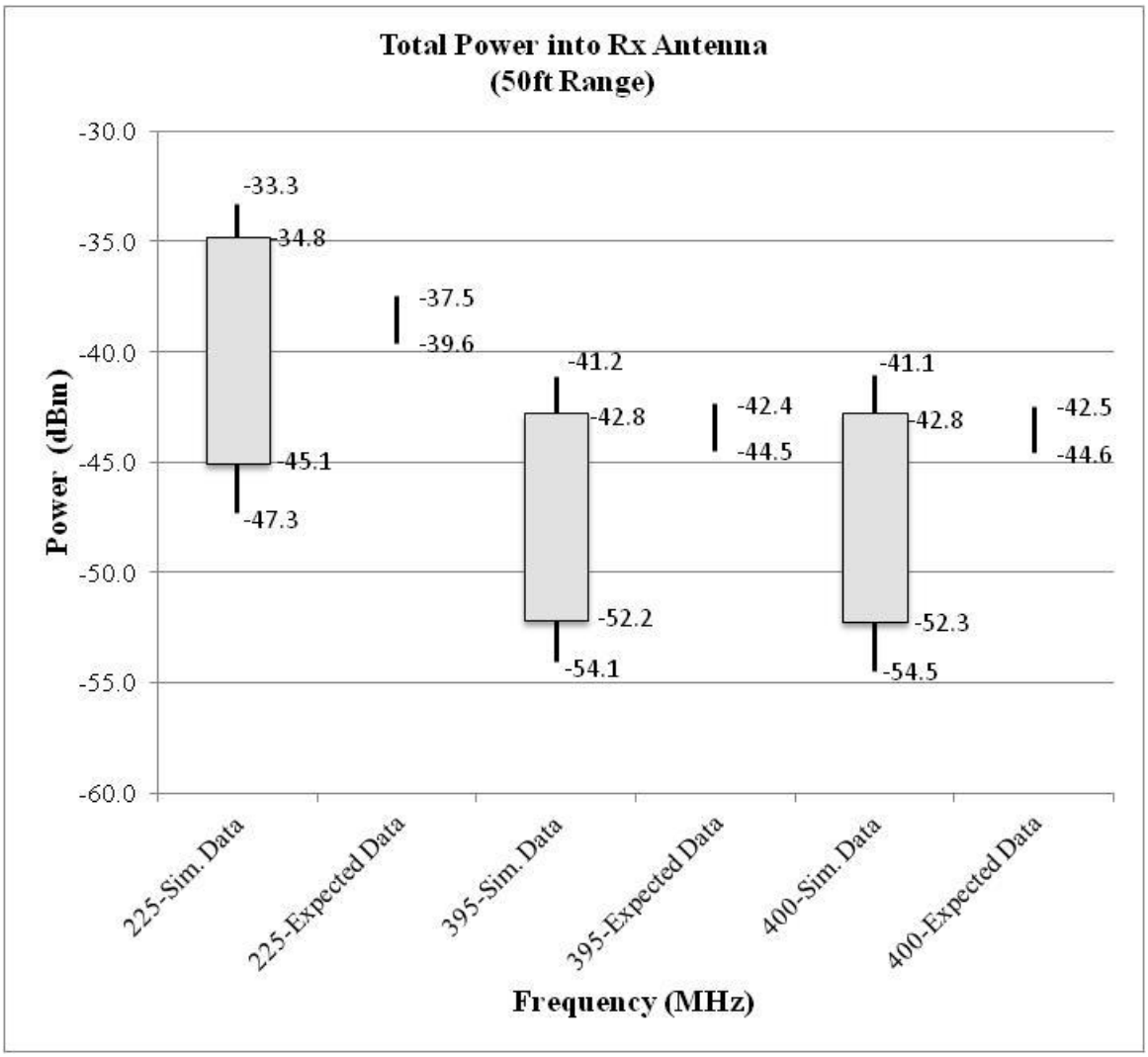

Figure 13: Total Power into Rx Antenna for 50ft Range

The range of simulated data for all frequencies was greater than that of the expected data. The simulated data ranges varied by frequency from 12.9 to 18.4dBm while the expected data ranges for all frequencies were only 2.1 dBm. Considering that the expected data was calculated using a single ray approach with consideration of only free space loss by distance and the simulation took into account multiple ray paths including transmission, reflections, and diffractions, greater data ranges for the simulation data was not surprising. While the range size varied, the simulation values and expected values did correspond with the simulation values overlapping expected values.

The simulation data for the 0.4Nmi slant range was plotted in a similar fashion alongside the revised expected data for comparison in the figure below. The ranges of the expected data were so minute particularly in comparison to simulation data ranges, that they were not represented as a line. Rather, their minimum and maximum were noted on the graph at the appropriate power level.

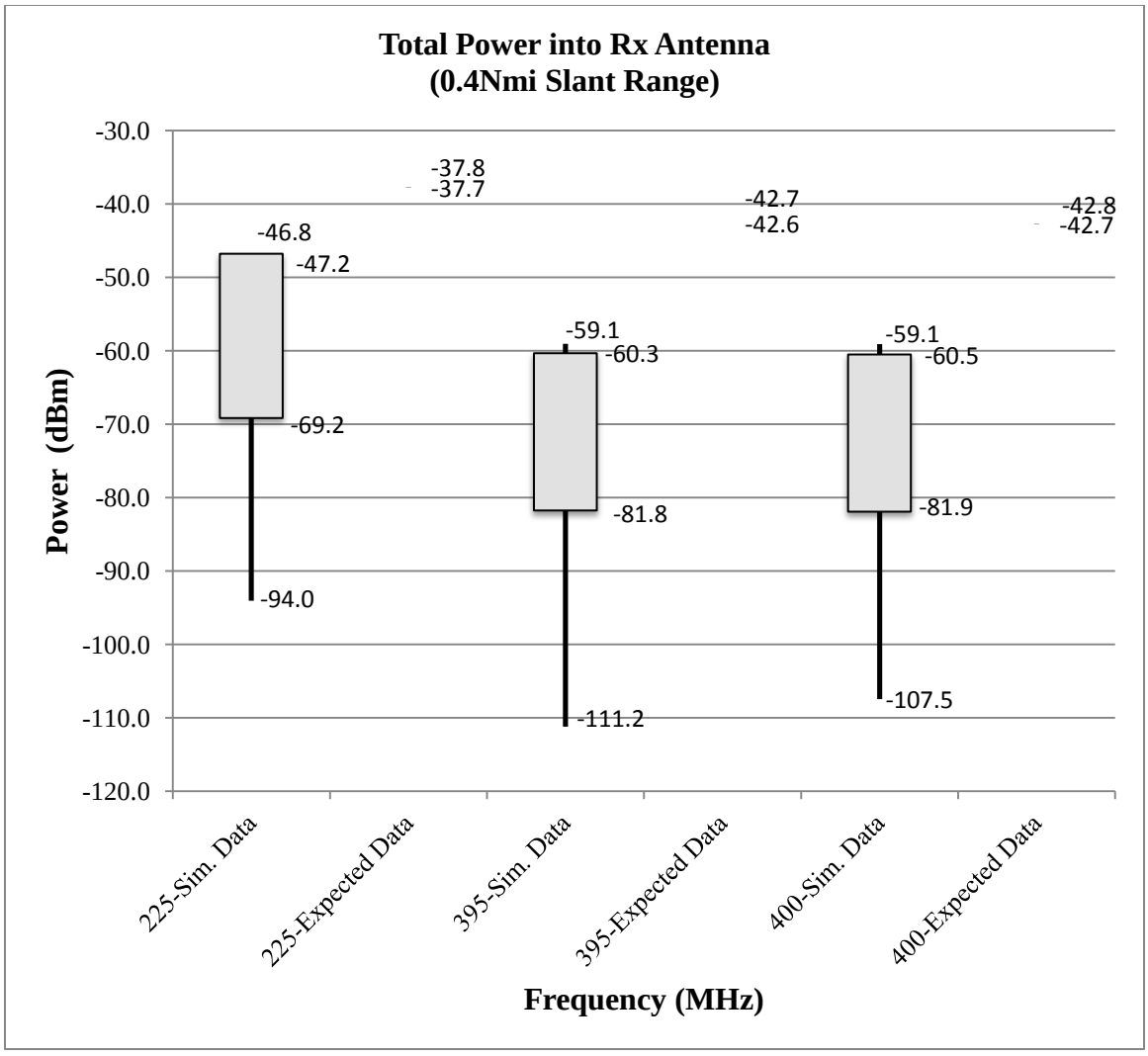

Figure 14: Total Power into Rx Antenna for 0.4Nmi Slant Range

Similar to the plot for the 50ft distance, the range for the simulation data was much greater than that of the expected data for the 0.4Nmi distance. However, the plots for the 0.4Nmi distance revealed some unique trends not seen for the shorter distance. First, the maximum values for the simulation data were 9.1 to 16.5dBm lower than the minimum values of the expected data. The simulation and expected values did not overlap at all. Second, the simulation values for the 0.4Nmi distance were weighted heavily toward the higher power levels. There was little variation between the maximums and averages including standard deviations by frequency. The minimums, however, appeared to be outliers as evident by the long extension of the minimum plot whiskers. While these data points appeared to be outliers, they were indicative of possible ray paths that could occur given similar conditions and valuable for the analysis.

Additional comparison of the data by approximate range distances is shown in the following table.

Table 5: Comparison of Data by Range Distance

Comparison of Data by Range Distance			
Frequency (MHz)	**Parameter (dBm)**	**50ft Range**	**0.4Nmi Slant Range**
225	$Data\ Range_{Sim}$-$Data\ Range_{Expected}$	11.8	46.8
	Max_{Sim}-$Max_{Expected}$	4.2	-9.5
	Min_{Sim}-$Min_{Expected}$	-7.7	-56.3
	Avg_{Sim}-$Avg_{Expected}$	-1.7	-32.9
395	$Data\ Range_{Sim}$-$Data\ Range_{Expected}$	10.8	52.1
	Max_{Sim}-$Max_{Expected}$	1.2	-16.4
	Min_{Sim}-$Min_{Expected}$	-9.5	-68.5
	Avg_{Sim}-$Avg_{Expected}$	-4.1	-42.5
400	$Data\ Range_{Sim}$-$Data\ Range_{Expected}$	13.4	48.4
	Max_{Sim}-$Max_{Expected}$	3.5	-16.4
	Min_{Sim}-$Min_{Expected}$	-9.9	-64.7
	Avg_{Sim}-$Avg_{Expected}$	-4.2	-40.5

In comparing the similarity of the simulation data to the expected data for the 50ft distance to the 0.4Nmi distance, it is evident that the data for the 0.4Nmi distance shows a much greater variation between that which was expected and that which was simulated for all parameters.

CHAPTER 6: CONCLUSIONS & RECOMMENDATIONS

The overall objective of this effort was to explore the supposition that an aircraft communications ground test with a relatively close range can adequately represent ground to air communications with a slant range of 0.4 nautical miles. A preliminary analysis and comparison of link budgets for both ranges was used to compensate for differences. For the 50ft range, power received via the aircraft antenna was fixed according to what was calculated for the 0.4Nmi range. Transmitter input power for the 50ft range was then varied from that of the 0.4Nmi range to compensate for differences in free space loss. The accuracy of this input power variation calculated using a single ray approximation was explored using simulations.

Data was calculated based upon an expected single direct transmission ray path and gathered through software simulations that included transmissions, reflections, diffractions, and multiple ray paths. All paths took into account free space loss. The original supposition was based upon only the calculation of the single direct transmission ray path.

While the basing initial analysis upon a single ray path is a good first approach to gather insight for basic transmission including free space path loss for that one ray, it neglects aspects of the environment that can contribute to the electromagnetic effects and overall resulting outcome. Comparison of expected data calculated using the single ray approach to the simulation incorporating multiple electromagnetic effects showed variations in received power for both scenarios of 50ft and 0.4Nmi. These variations were not consistent in magnitude between the 50ft range scenario and 0.4Nmi slant range scenario. The comparative deviations were significantly greater for the 0.4Nmi slant range, thereby affecting the accuracy of extrapolating results of a 50ft single ray approach to that of a 0.4Nmi slant range. While valuable for an initial evaluation, the close range test does not replace the complexity and value of test at actual range distance. Furthermore, while the simulation of static features does take into account a number of additional factors, it does not replace the dynamic environment of an actual flight test. The results of this project lend support to the value of comprehensive testing incremented with building complexity.

It is recommended that the ground test take into account the received power variations demonstrated by the simulations for a more thorough test. With the minimum received power of -111.2dBm from the simulations, the revised minimum EIRP would be -63.2dBm for the 50ft ground test range. The ground test should incorporate incrementally decreasing input powers from 5.3dBm derived from the single ray approximation to -111.2dBm gleaned from incorporating additional electromagnetic effects within the simulations. The previously presented link budget has been revised for the 50ft range and is shown as follows.

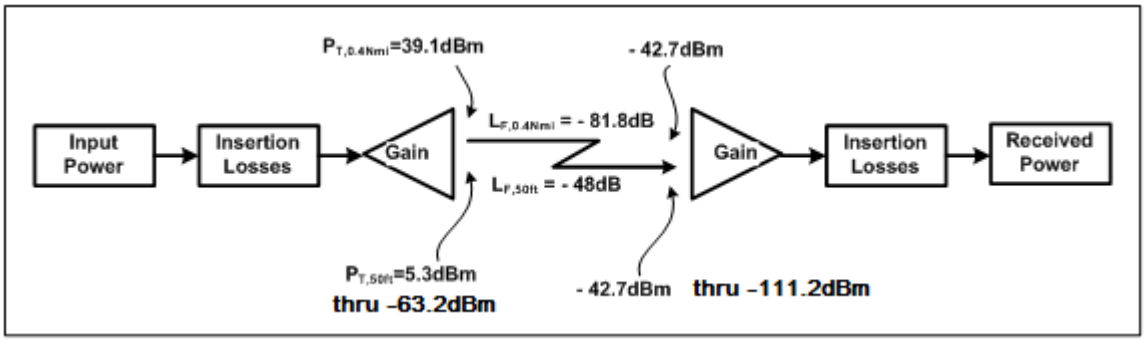

Figure 15: Revised Link Budget for 50ft Range

REFERENCES

1) Ahirwar, S.D, C. Sairam, Ashwani Kumar, *Broadband Blade Monopole Antenna Covering 100-2000 MHz Frequency Band*, Defense Electronics Research Laboratory, 2009.

2) Cheng, David K., *Field and Wave Electromagnetics*, 2nd Edition, Addison Wesley, 1992.

3) Evans, R.W., *Design Guidelines for Shielding Effectiveness, Current Carrying Capability, and the Enhancement of Conductivity of Composite Materials*, NASA: Marshall Space Flight Center, August 1997.

4) Felbecker, Robert, et al., *Estimation of Effective Permittivity and Effective Thickness of Inhomogeneous Materials at 52-70GHz*, German Federal Ministry of Education and Research and Airbus, 2009.

5) Hemming, Leland H., *Electromagnetic Anechoic Chambers, Appendix A.2: Fresnel Zone Analysis*, Wiley-Interscience, 2002.

6) Hollis, J.S., et al., *Microwave Antenna Measurements*, Scientific Atlanta, 1985.

7) *IEEE Std 149-1979 (R2008): Standard Test Procedures for Antennas*, Antenna Standards Committee.

8) Stutzman, Warren L., Gary Thiele, *Antenna Theory and Design*, Wiley & sons, 1998.

9) Volakis, John L., *Antenna Engineering Handbook, Chapter 40: Aircraft Antennas*, McGraw Hill, 2007.

10) *XGTD: General Purpose Ray-Based Electromagnetic Analysis Software, User's Manual*, Version 2.5, Remcom, 2010.

APPENDIX A – Fresnel Zones

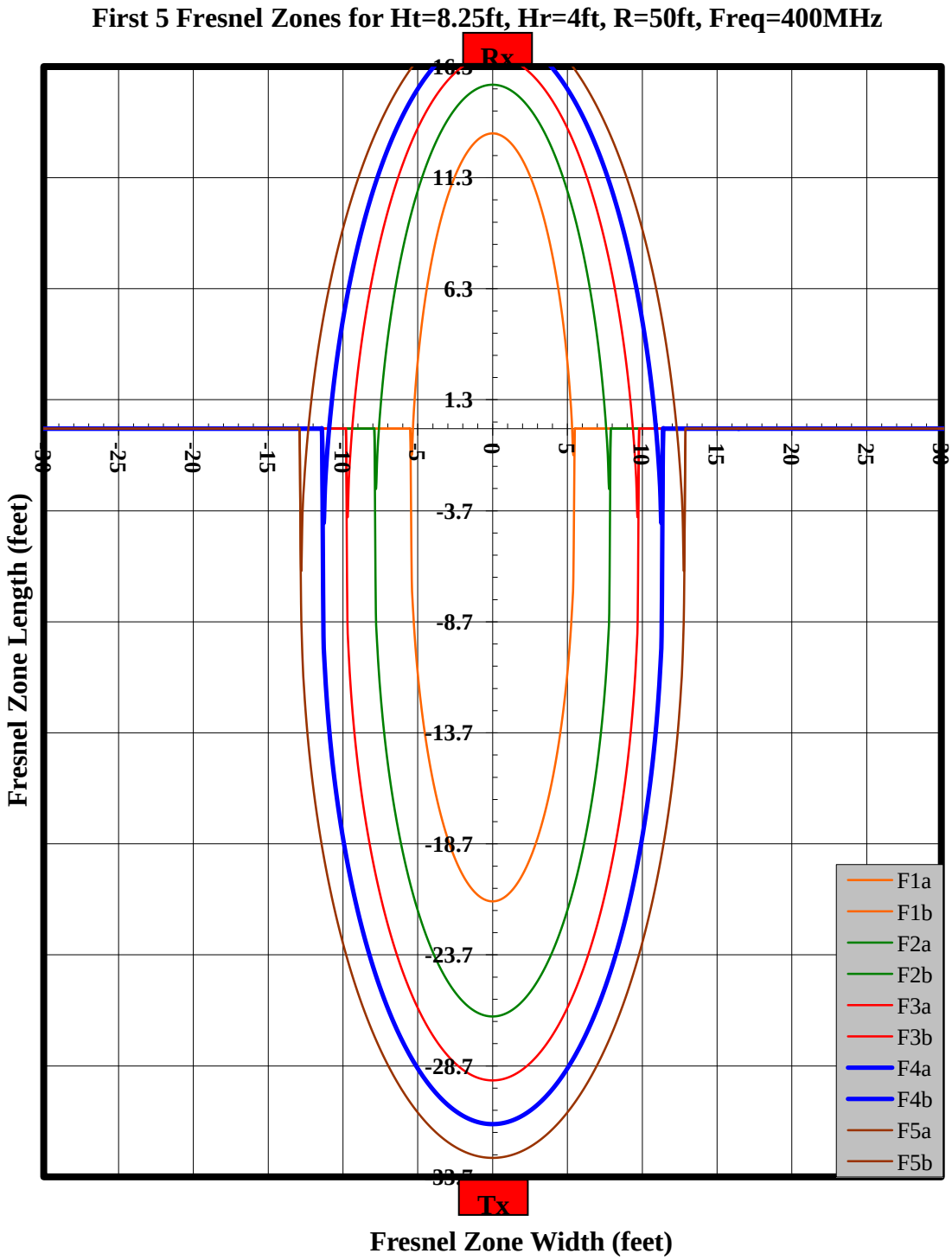

Figure 16: Fresnel Zones for 50ft Range at 400MHz

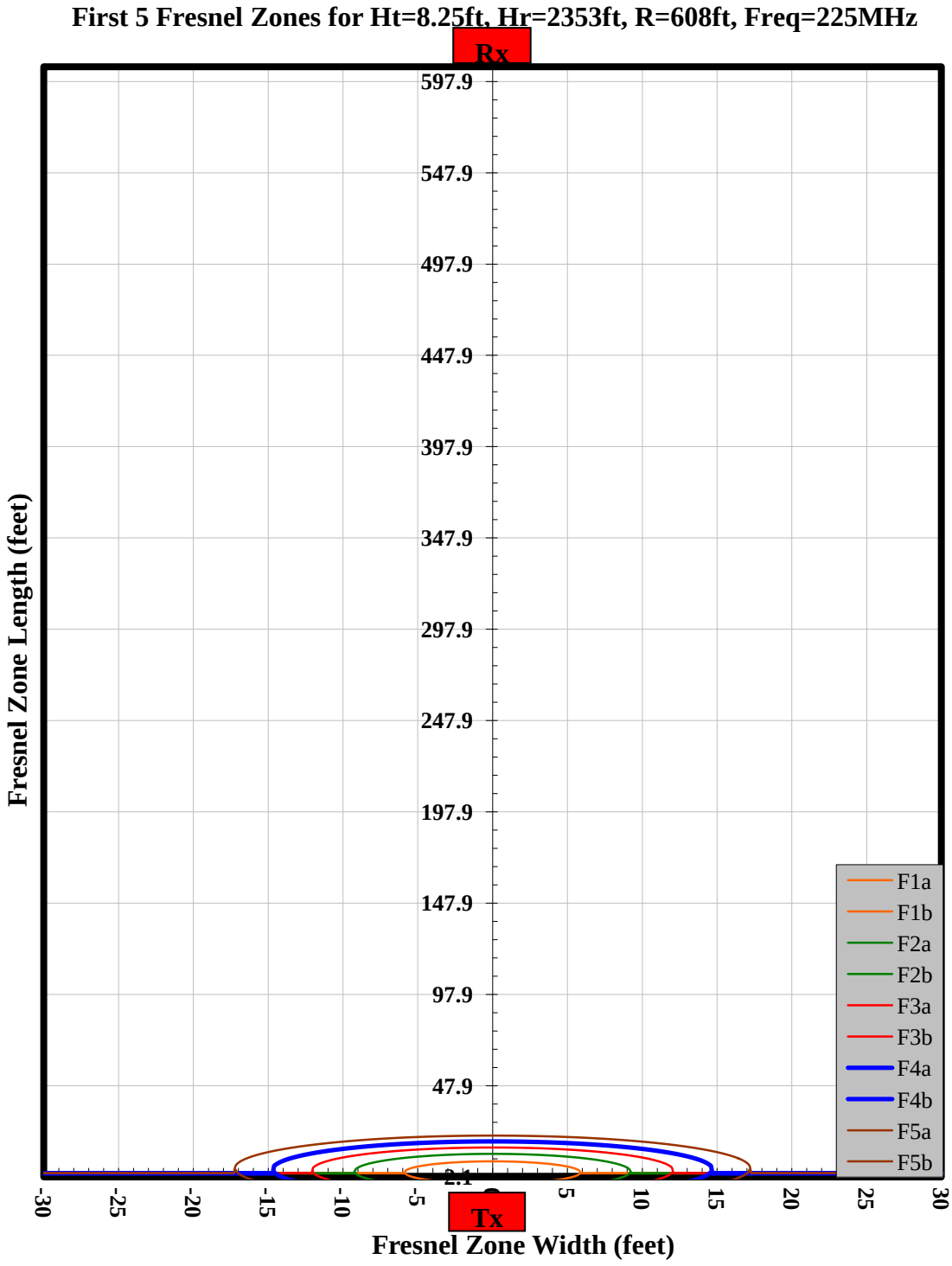

Figure 17: Fresnel Zones for 608ft Range & 0.4 Slant Range at 225MHz

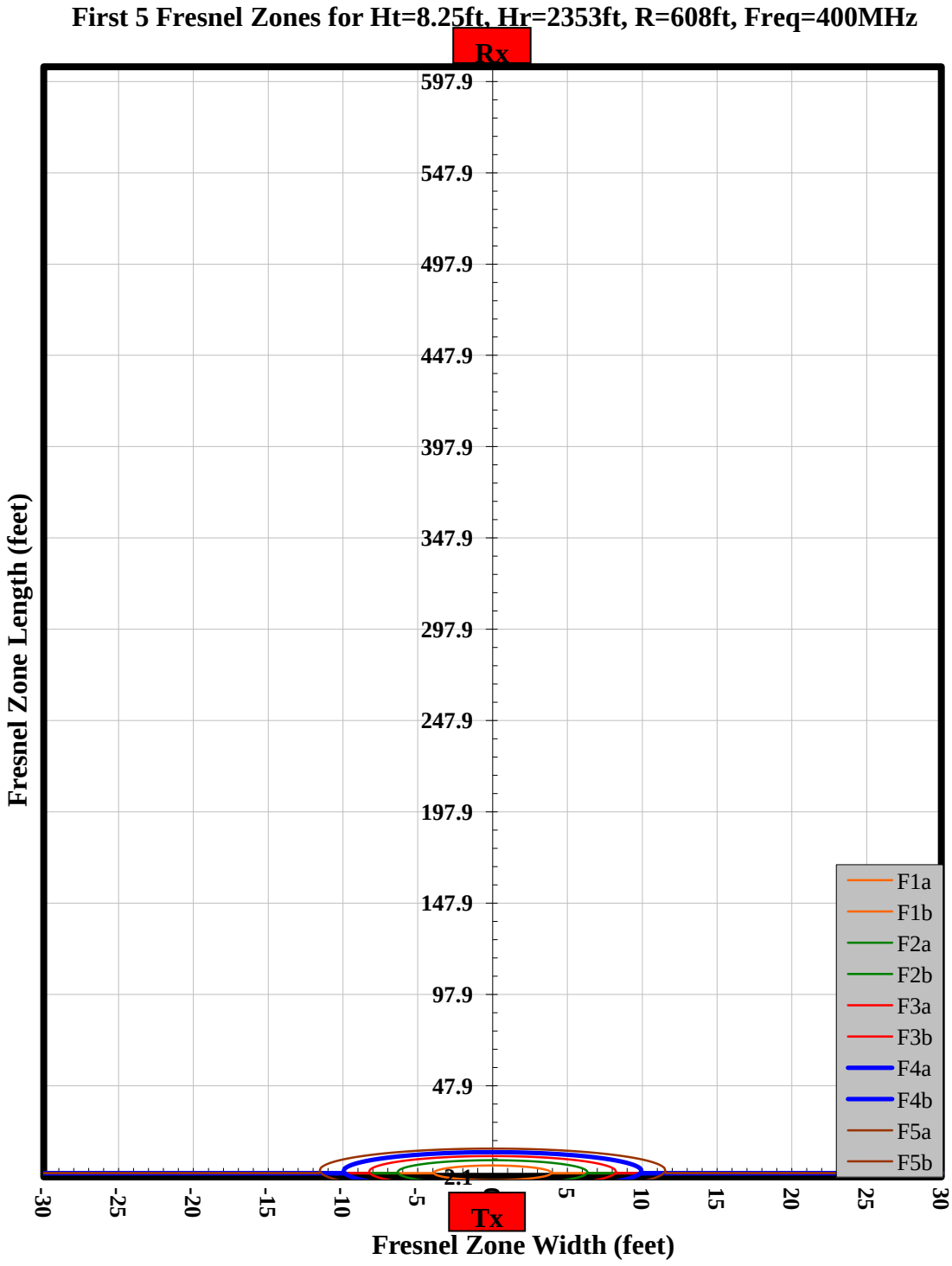

Figure 18: Fresnel Zones for 608ft Range and 0.4Nmi Slant Range at 400MHz

APPENDIX B – Graphical Data

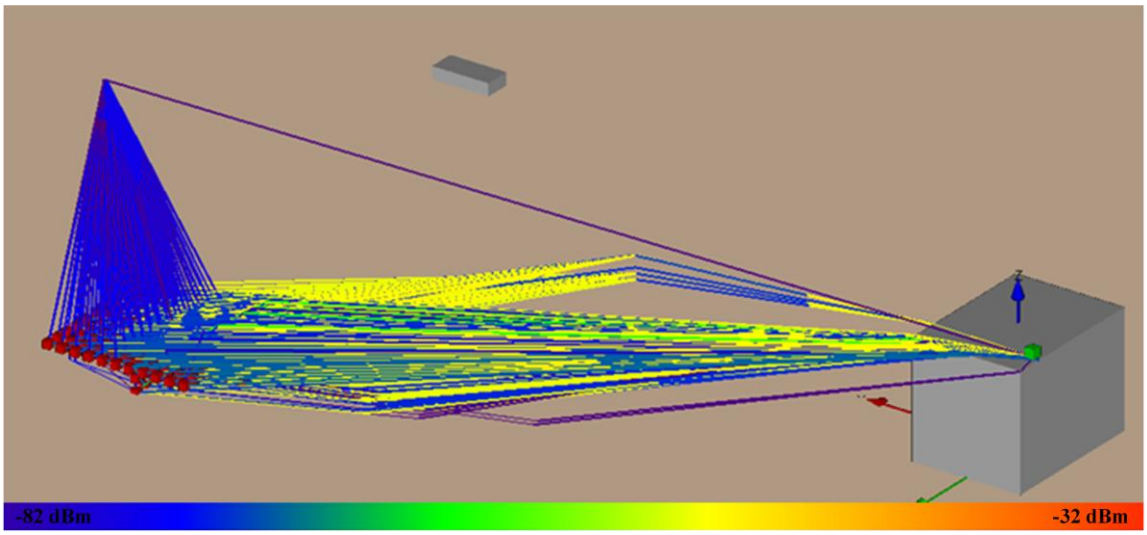

Figure 19: Propagation Paths for 50ft Range and 395MHz

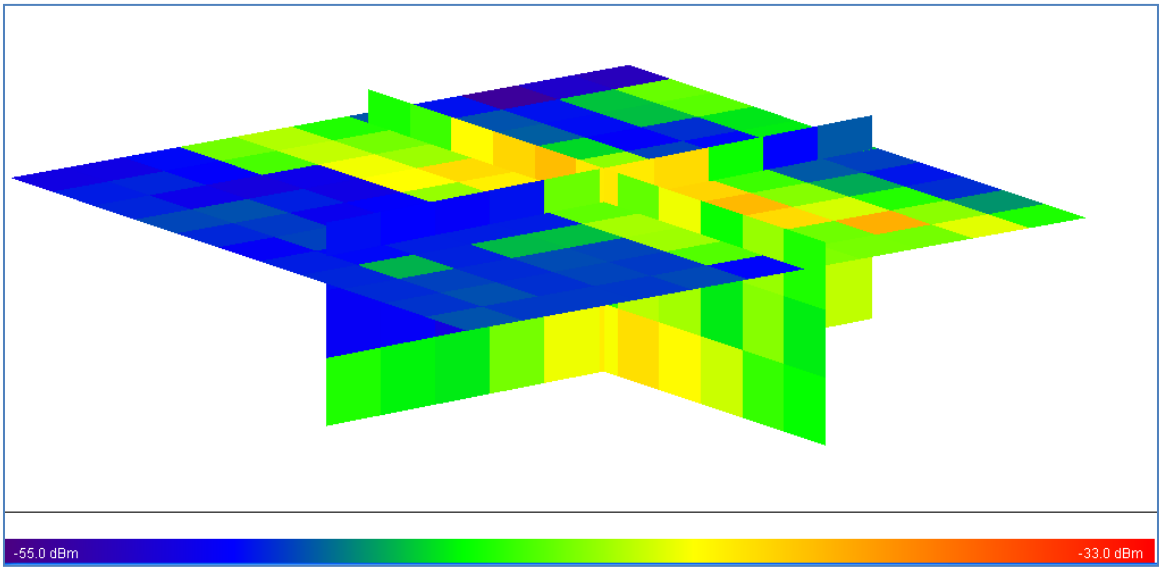

Figure 20: Received Power for 50ft Range and 395MHz

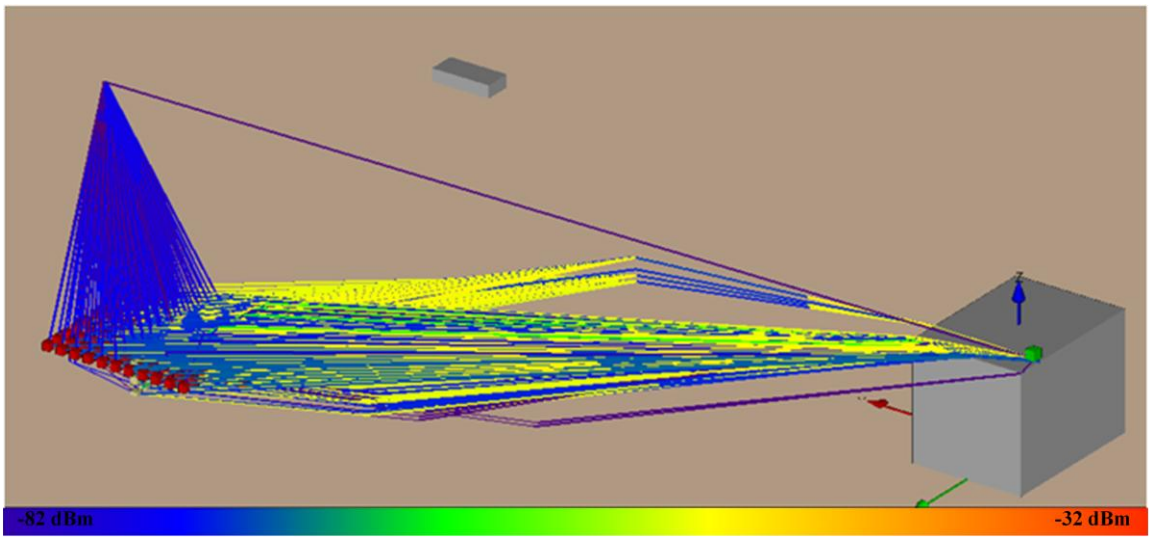

Figure 21: Propagation Paths for 50ft Range and 400MHz

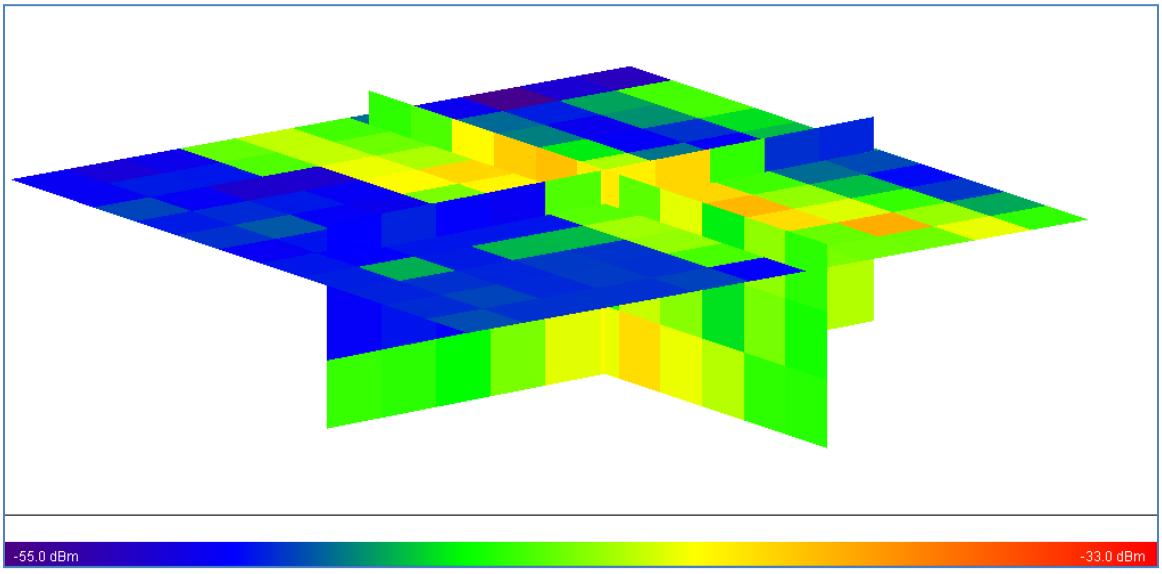

Figure 22: Received Power for 50ft Range and 400MHz

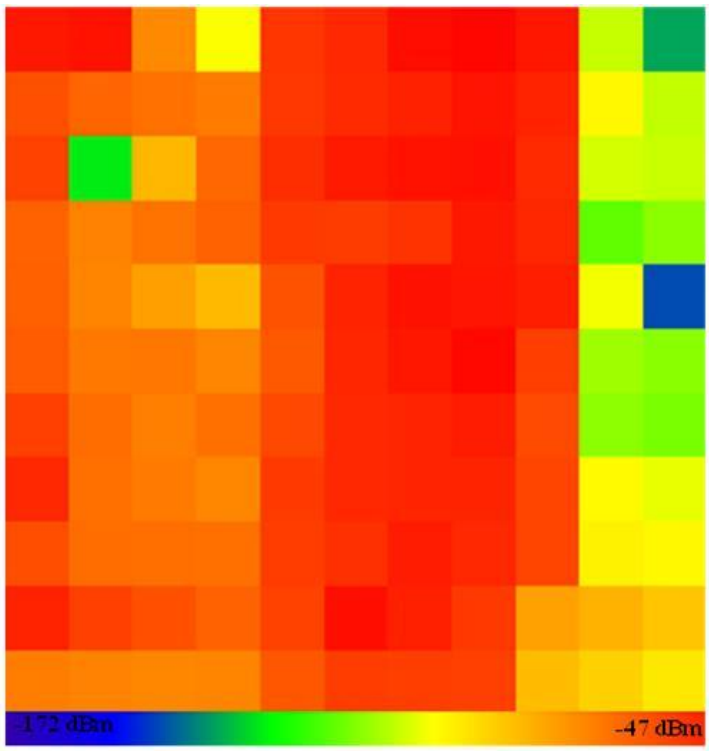

Figure 23: Received Power for 0.4Nmi Range and 225MHz

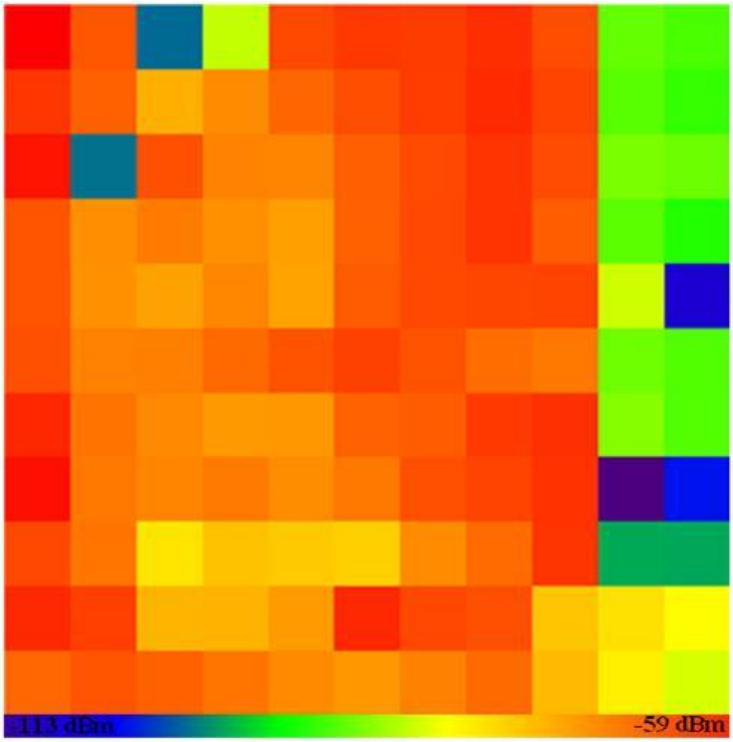

Figure 24: Received Power for 0.4Nmi Range and 395MHz

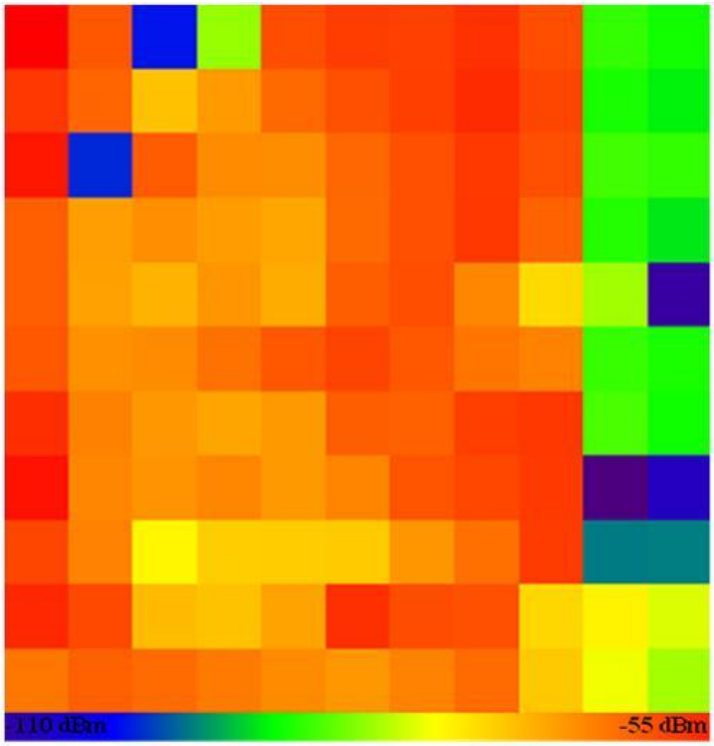

Figure 25: Received Power for 0.4Nmi Range and 400MHz

APPENDIX C – Power vs. Distance Plots

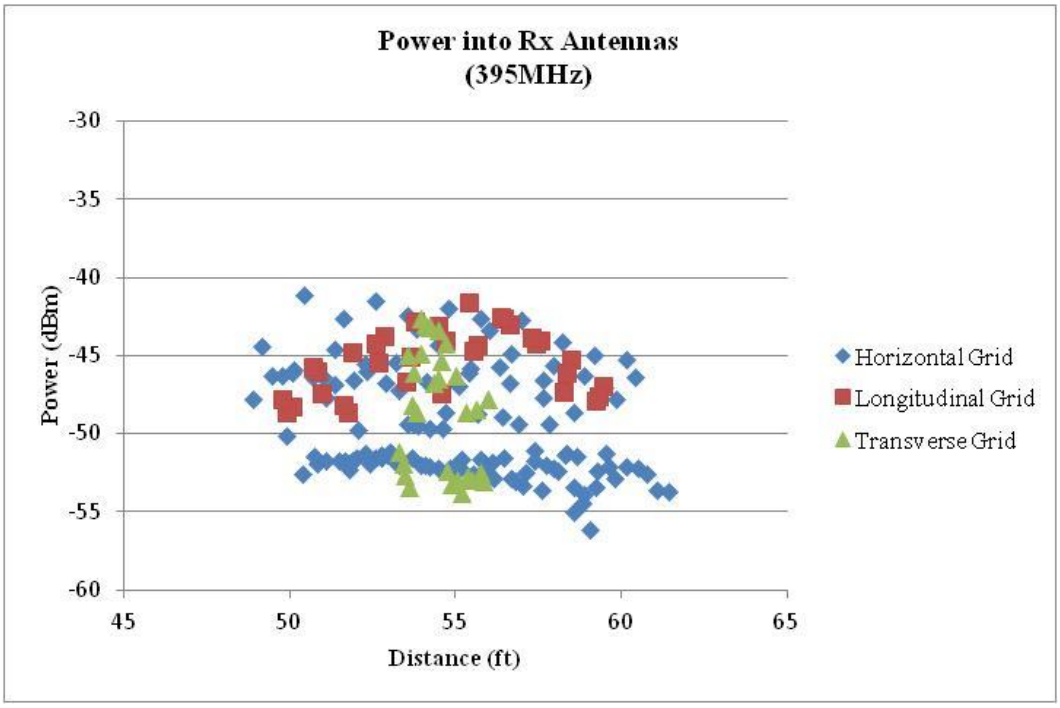

Figure 26: Power vs. Distance for ~50ft Range and 395MHz

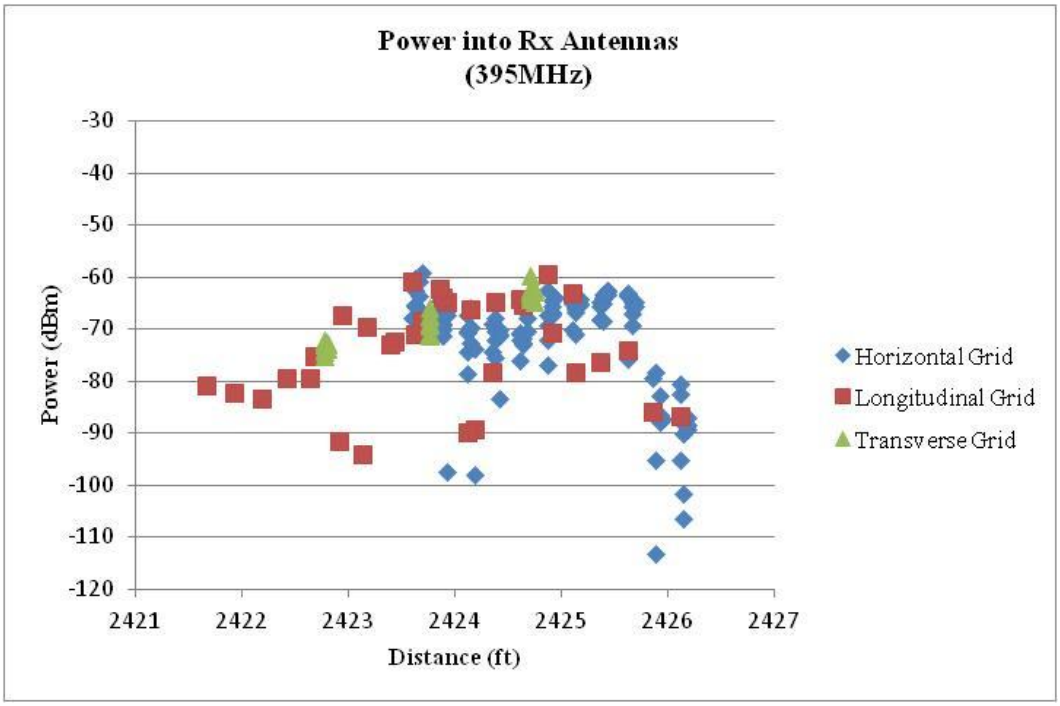

Figure 27: Power vs. Distance for ~0.4Nmi Slant Range and 395MHz

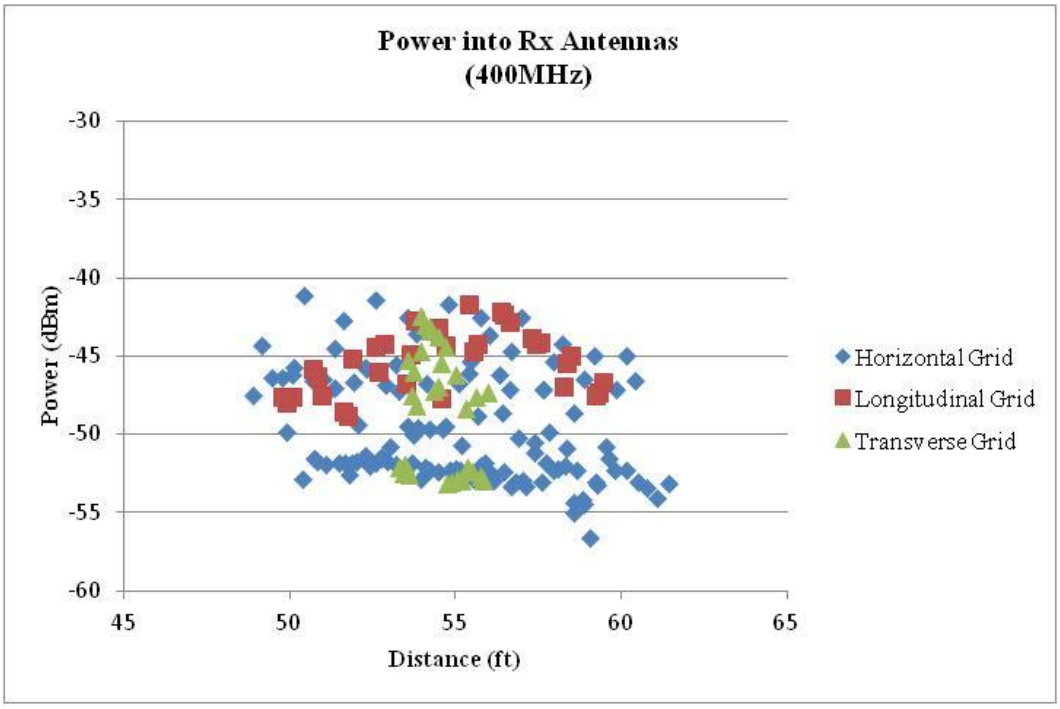

Figure 28: Power vs. Distance for ~50ft Range and 400MHz

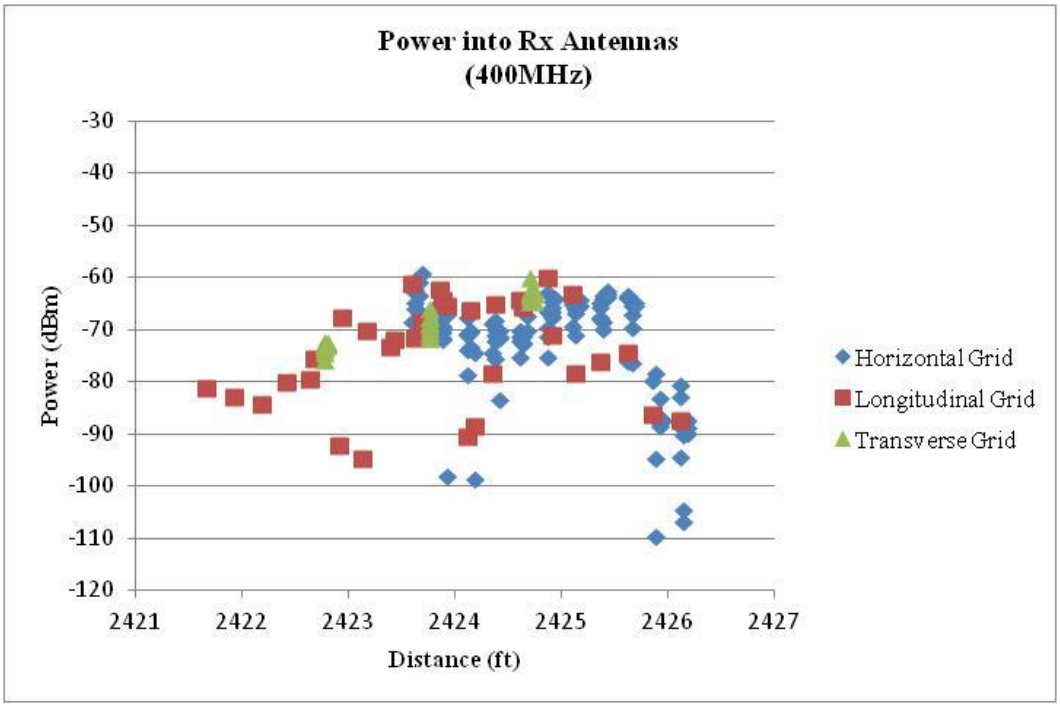

Figure 29: Power vs. Distance for ~0.4Nmi Slant Range and 400MHz

APPENDIX D – Receiver Grids

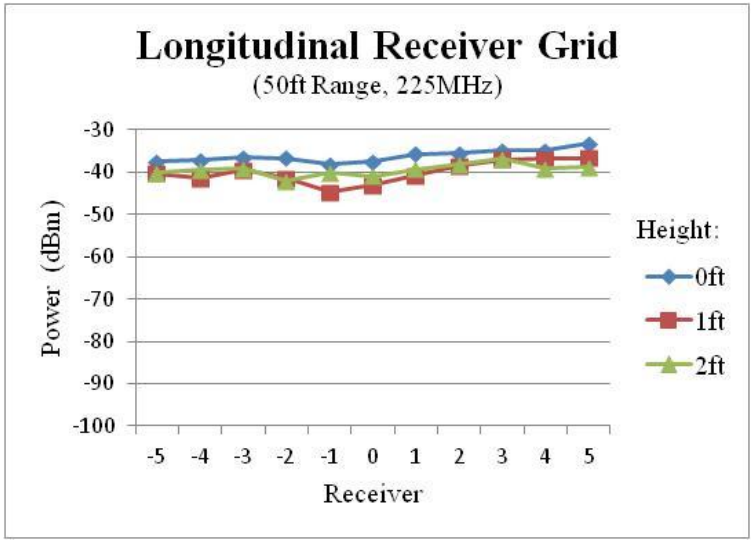

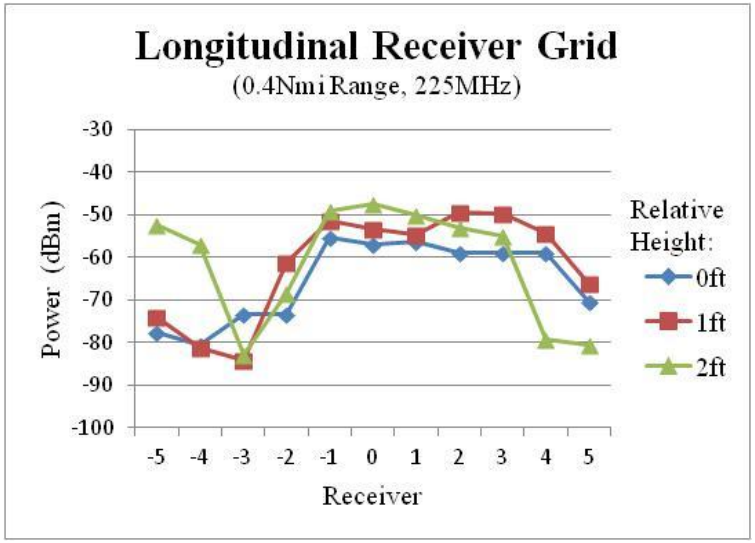

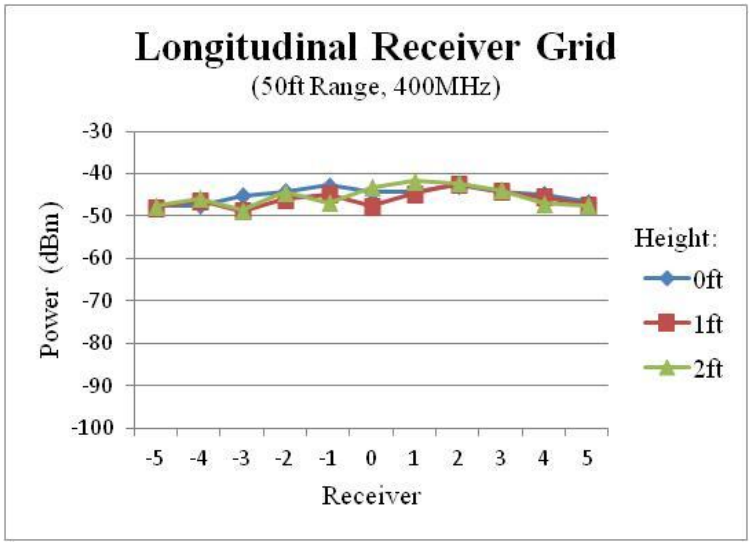

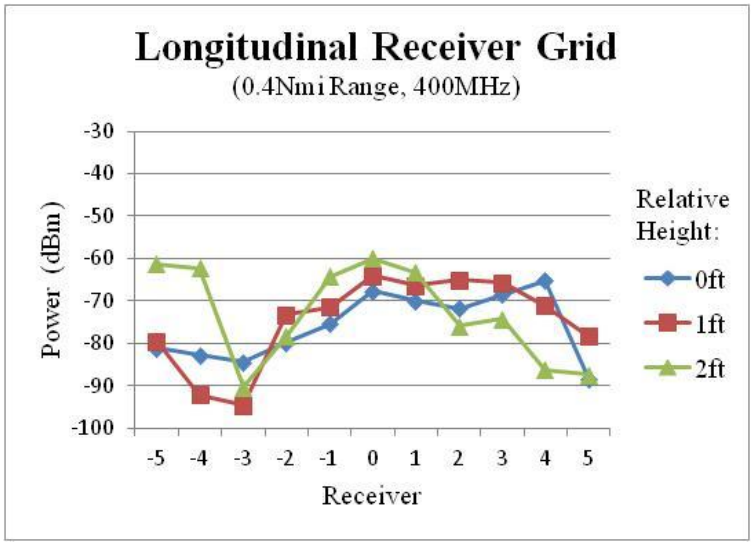

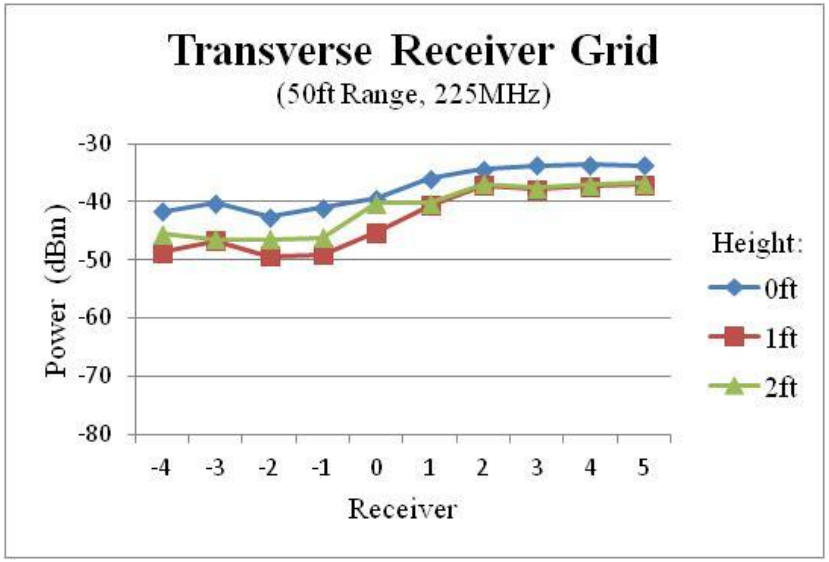
Transverse Receiver Grid
(50ft Range, 225MHz)
Power (dBm)
-30
-40
-50
-60
-70
-80
-4 -3 -2 -1 0 1 2 3 4 5
Receiver
Height:
0ft
1ft
2ft

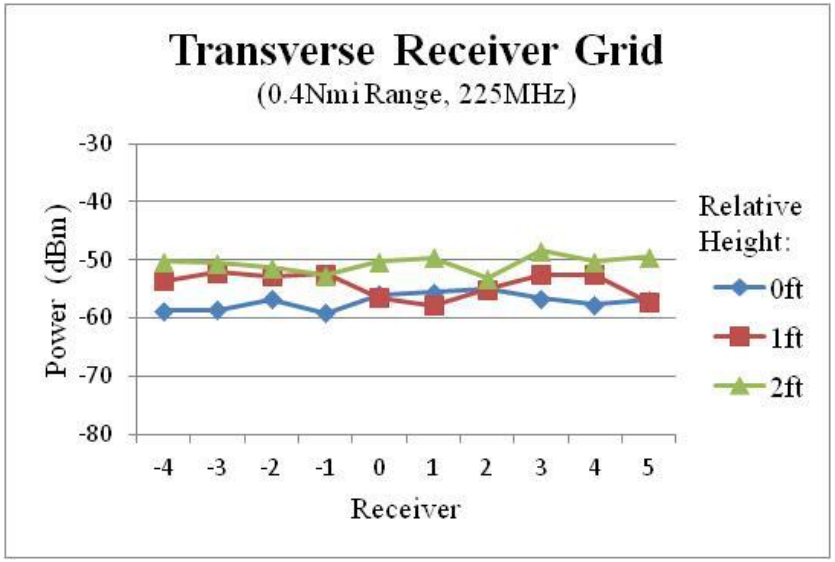
Transverse Receiver Grid
(0.4Nmi Range, 225MHz)
Power (dBm)
-30
-40
-50
-60
-70
-80
-4 -3 -2 -1 0 1 2 3 4 5
Receiver
Relative
Height:
0ft
1ft
2ft


Transverse Receiver Grid
(50ft Range, 400MHz)
Power (dBm)
-30
-40
-50
-60
-70
-80
-4 -3 -2 -1 0 1 2 3 4 5
Receiver
Height:
0ft
1ft
2ft

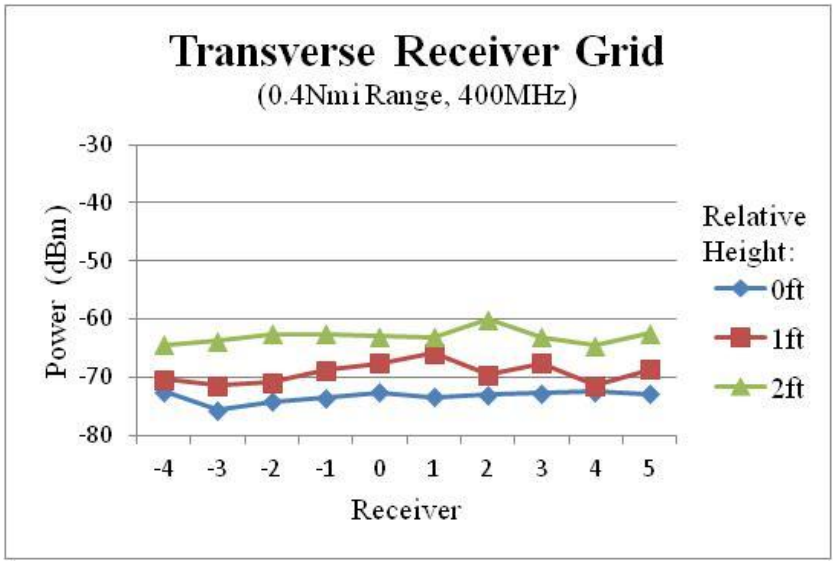
Transverse Receiver Grid
(0.4Nmi Range, 400MHz)
Power (dBm)
-30
-40
-50
-60
-70
-80
-4 -3 -2 -1 0 1 2 3 4 5
Receiver
Relative
Height:
0ft
1ft
2ft

APPENDIX E – List of Abbreviations and Acronyms

All abbreviations, acronyms, and symbols used in the report, including those in figures, tables, and the appendices, are listed alphabetically in this appendix.

Abbreviation	Definition
AC	Aircraft
Aircraft Comm	Aircraft Communications
CATE	Common Airborne Test Equipment
DAP	Data Analysis Plan
dB	Decibels
dBm	Decibels referenced to a milliwatt
ERP	Effective Radiated Power
GS1	Ground Station 1
GS2	Ground Station 2
Gtd	Geometric Theory of Diffraction
Hr	Height, Receiver Antenna
Ht	Height, Transmitter Antenna
LOS	Line of Sight
MHz	Megahertz
Nmi	Nautical Miles
Rx	Receive
Tx	Transmit
UHF	Ultra High Frequency